Journal of ELECTRONIC MATERIALS, Vol. 48, No. 10, 2019
https://doi.org/10.1007/s11664-019-07289-1

Full-Wafer Strain and Relaxation Mapping of $Hg_{1-x}Cd_xTe$ Multilayer Structures Grown on $Cd_{1-y}Zn_yTe$ Substrates

B. SHOJAEI ,[1,2] R. COTTIER,[1] D. LEE,[1] E. PIQUETTE,[1] M. CARMODY,[1] M. ZANDIAN,[1] and A. YULIUS[1]

1.—Teledyne Scientific and Imaging, Camarillo, CA 93012, USA. 2.—e-mail: Bo.Shojaei@Teledyne.com

State-of-the-art $Hg_{1-x}Cd_xTe$ multilayer structures grown by molecular beam epitaxy on (211)-oriented $Cd_{1-y}Zn_yTe$ substrates have been characterized and their strain and relaxation analyzed. Techniques for measuring lattice mismatch, strain, and crystal quality by measuring symmetric and asymmetric diffraction profiles in different azimuths were adapted and performed in combination with dislocation delineation for full-wafer and multilayer characterization. It was found that the degree of lattice mismatch and in turn the strain state of epitaxial multilayers can be made uniform across full wafers in optimized structures. A strong correlation was revealed between the Zn composition of the $Cd_{1-y}Zn_yTe$ substrates and the crystal quality of the active layers in the multilayer structures. This method can be generalized to optimize multilayer structures to minimize relaxation by the generation of extended defects.

Key words: HgCdTe, molecular beam epitaxy, strain, dislocations, fully depleted infrared detectors

INTRODUCTION

In recent years, Teledyne has positioned itself to push the boundaries of two aspects of infrared detector technology: high-performance large-area detectors[1] and fully depleted *p-v-n* planar heterojunction detectors having dark currents limited by background radiation rather than Auger-1 recombination.[2] Achieving these technological milestones will have a significant impact on civil, space, and defense applications, and thus far, advances have been enabled by improvements in $Hg_{1-x}Cd_xTe$ infrared materials grown by molecular beam epitaxy (MBE) and detector fabrication.

As $Hg_{1-x}Cd_xTe$ detectors approach background-radiation-limited performance and detector arrays increase in size, the required detector material areal uniformity that results in desired detector operability becomes more challenging to achieve. Detector material inhomogeneity may arise from the substrate on which thin films are grown, from the MBE growth process, and from the fabrication processes that produce focal-plane arrays. Consequences of inhomogeneity in the detector material include variations in strain and relaxation by the formation of extended defects, namely dislocations, in the epitaxial multilayers.

There is ample experimental evidence that dislocations diminish the performance of HgCdTe detectors.[3–5] Dislocations may reduce minority-carrier lifetime by acting as Shockley–Read–Hall recombination centers, and when in or near the junction region, may enable tunneling currents. It is interesting to note the sensitivity of the zero-bias impedance (R_0A product) to the dislocation density;[5] it is plausible that fully depleted detectors in which the relative portion of the device volume having an increased screening length is larger will have greater sensitivity to charged dislocations at low temperatures. Large-area and fully depleted detector performance will benefit from minimizing the formation of extended defects.

(Received November 30, 2018; accepted May 14, 2019; published online May 23, 2019)

There are numerous sources of dislocation generation during the epitaxy of and subsequent photodiode detector fabrication on $Hg_{1-x}Cd_xTe$ grown on $Cd_{1-y}Zn_yTe$ substrates.[6–10] The principal mechanism of dislocation formation relevant to this work is that due to the lattice mismatch between HgTe, CdTe, ZnTe, and their alloys. State-of-the-art $Hg_{1-x}Cd_xTe$ photodetectors are grown by MBE on nearly lattice-matched $Cd_{1-y}Zn_yTe$ substrates to minimize the formation of extended defects. A single epitaxial film of $Hg_{1-x}Cd_xTe$ can be grown on a lattice-matched $Cd_{1-y}Zn_yTe$ substrate if the compositions, x and y, of the respective layers are chosen such that the lattice parameters of the alloys are equal. In this case, an epitaxial layer will grow without introducing additional defects. If there is a misfit between the layers, the $Hg_{1-x}Cd_xTe$ will grow strained, and for a sufficient misfit at a given thickness, or a sufficient thickness at a given misfit, the stress in the film will create extended defects to minimize the free energy of the system.[11]

A multilayer epitaxial system of $Hg_{1-x}Cd_xTe$ grown on a $Cd_{1-y}Zn_yTe$ substrate cannot be perfectly lattice matched. Such a structure will have a strain profile that is dependent on the lattice parameters of the individual layers, the lattice parameter of the substrate, the degree to which the structure relaxes, and where in the structure relaxation takes place. Predictions for the onset of relaxation can be made by calculations of the excess stress,[12] a force balance between the dislocation line tension and the in-plane misfit stress, in the film for various types of dislocations and considering both single- and double-kink relaxation. Phenomenological models can enable such calculations to approximate the effect of time and temperature on defect generation.[13] However, thermodynamic models that predict whether a structure is stable or not against bending, elongation, and formation of dislocations have critical shortcomings; For example, they do not account for kinetic barriers, they typically neglect the effect of the presence of dislocations, and they do not account for the relaxation of the structure as the film is grown. In practice, it is difficult to predict the mismatch that would cause the formation of dislocations in multilayer structures.

The two following questions are posed: (1) What degree of mismatch can a given multilayer structure afford before forming a significant number of dislocations? (2) For a given multilayer structure, what is the optimal lattice parameter of the substrate? This work addresses these questions by the characterization and analysis of strain and relaxation in state-of-the-art $Hg_{1-x}Cd_xTe$ multilayer structures grown by molecular beam epitaxy on (211)-oriented $Cd_{1-y}Zn_yTe$ substrates. The techniques developed for measuring lattice mismatch, tensile and shear strain by measuring symmetric and asymmetric diffraction profiles in different azimuths[14–16] were adapted and performed in combination with dislocation delineation for multilayer structure and full-wafer characterization. It was found that the degree of lattice mismatch and in turn the strain state of epitaxial multilayers can be made uniform across full wafers in optimized structures. A method of mapping the crystalline quality by measurements of the full-width at half-maximum (FWHM) of double-crystal rocking curves[17] was adapted for characterization of multilayer structures. A strong correlation was observed between the Zn composition of the $Cd_{1-y}Zn_yTe$ substrates and the crystal quality of the active layers in the multilayer structures. These methods can be generalized to optimize structures to minimize relaxation by the generation of extended defects.

EXPERIMENTAL PROCEDURES

Multilayer $Hg_{1-x}Cd_xTe$ structures were grown on (211)-oriented $Cd_{1-y}Zn_yTe$ substrates in a RIBER 32P MBE system. The precise composition of the structures cannot be disclosed, but the active layer of the structures was of suitable composition and thickness for detection of long-wave infrared (LWIR) radiation. The substrates were provided by a supplier regarded by many as that which produces the highest-quality $Cd_{1-y}Zn_yTe$. The Zn composition of the substrates varied within and between substrates, and the supplier provided the Zn composition as a function of position on the substrate. In select cases, the composition provided by the supplier was verified using Bond's method.[18]

The general measurement technique involved recording an x-ray diffraction intensity profile from the surface symmetric (422) reflection from a LWIR $Hg_{1-x}Cd_xTe$ multilayer structure at an array of points across the $Cd_{1-y}Zn_yTe$ substrate at which the Zn composition was known. At select points, surface symmetric and asymmetric (440, 404, 511, and 333) reciprocal-space maps (RSMs) were recorded and/or defect delineation by a wet chemical etch was performed to determine the strain state and the degree of relaxation by the formation of defects, respectively. Having knowledge of the Zn composition of the substrate at which measurements were performed on the $Hg_{1-x}Cd_xTe$ multilayer structures allowed the correlation between the reflection peak widths, the strain state, and the defect densities with the composition of the substrate.

X-ray diffraction measurements were performed on a Rigaku SmartLab high-resolution x-ray diffractometer system with a four-crystal Ge monochromator and using Cu K_α radiation. The monochromator used the Ge (440) reflection, giving beam divergence of 4 arcseconds. A computer controlled the goniometer and sample stage degrees of freedom, viz. the angle of incidence (ω), scattering angle (2K), sample rotation about the surface normal (φ), sample tilt (χ), and sample translation (x, y). Slits were chosen such that the beam spot size on the sample was 1 mm × 2 mm. The diffracted beam was collected by a wide-aperture detector. To

determine distortions of the crystalline lattice, a Ge (220) analyzer was added to the instrument to construct high-resolution reciprocal-space maps. Sample alignment and data acquisition were automated using Rigaku's instrument control software.

RESULTS AND DISCUSSION

An example dataset that maps the substrate Zn composition and the FWHM of the (422) x-ray diffraction reflection from the active layer of a LWIR $Hg_{1-x}Cd_xTe$ multilayer structure is shown in Fig. 1a and b, respectively. The intensity of the incident and diffracted beam decreases with depth and is a function of the angle of incidence and exit. This can affect the absolute resolution of crystal quality measurements. The effect on the measurements of the buried layers was small and, importantly, did not prevent the establishment of the dependence of the crystal quality on the composition of the substrate. The maps clearly indicate a correlation between the measured FWHM from the multilayer structure and the Zn composition of the substrate. Where the FWHM was smaller indicates where the crystal quality of the multilayer structure was relatively better. On this wafer, the highest crystal quality was obtained where the Zn composition was 4.0% to 4.1%.

The correlation between the substrate Zn composition and the crystal quality of the $Hg_{1-x}Cd_xTe$ multilayer structure was measured over a larger Zn composition range than depicted in Fig. 1 by growing nominally identical structures on multiple substrates. Figure 2 depicts the dependence of the FWHM of the (422) x-ray diffraction reflection from the active layer of seven LWIR $Hg_{1-x}Cd_xTe$ multilayer structures. The films were grown consecutively and in a single growth campaign to avoid run-to-run variations. Furthermore, the void density was lower than 800 cm^{-2} and the microvoid density was lower than 5000 cm^{-2} over the entire mapped region of each wafer, with levels generally at or near the limits imposed by the substrates.[19] The variation of the $Hg_{1-x}Cd_xTe$ composition was less than 0.01 in absolute composition over the entire mapped region of each wafer.

In Fig. 2, higher crystal quality corresponds to lower FWHM, and smaller lattice parameter corresponds to larger percent Zn composition. The dataset indicates that, for the particular structure under investigation, optimal crystal quality was obtained when the Zn composition of the substrate was in the vicinity of 4.3%.

To determine the extent to which the films were relaxing by the formation of extended defects due to lattice mismatch with the substrate, a strip was cleaved from each wafer and sections of the strips were exposed to a dislocation decoration wet chemical etch. Figure 3 shows scanning electron microscopy micrographs measured on the [01-1] face of several LWIR $Hg_{1-x}Cd_xTe$ multilayer structures grown on (211)-oriented $Cd_{1-y}Zn_yTe$ substrates after the dislocation decoration etch was performed. The micrographs are labeled 1 to 5 in order of increasing strain of the $Hg_{1-x}Cd_xTe$ multilayer structure with respect to the substrate. The

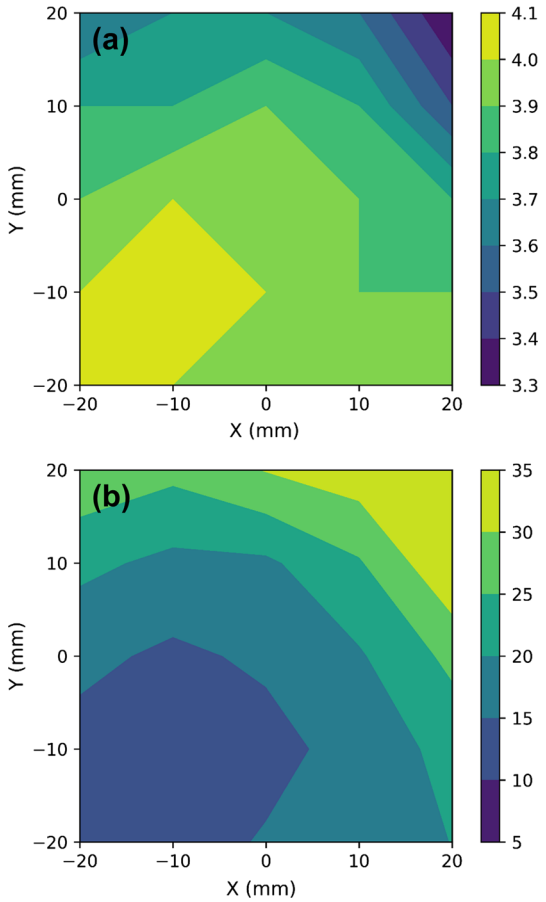

Fig. 1. (a) Map of percent Zn composition as function of position on (211)-oriented $Cd_{1-y}Zn_yTe$ substrate. (b) Map of full-width at half-maximum measured in arcseconds as a function of position of the (422) x-ray diffraction reflection from the active layer of a LWIR $Hg_{1-x}Cd_xTe$ multilayer structure grown on the substrate in (a).

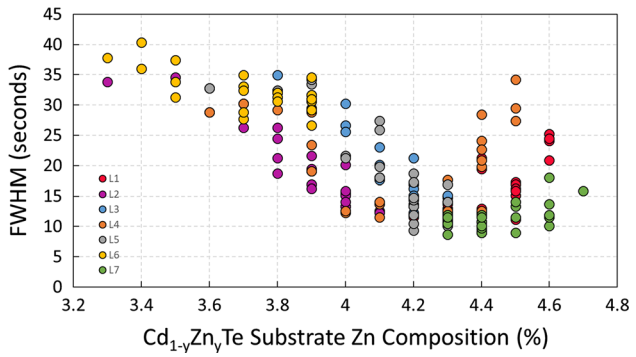

Fig. 2. The full-width at half-maximum of the surface symmetric (422) x-ray diffraction reflection from the active layer of seven nominally identical LWIR $Hg_{1-x}Cd_xTe$ multilayer structures versus the Zn composition of the (211)-oriented $Cd_{1-y}Zn_yTe$ substrates on which the structures were grown.

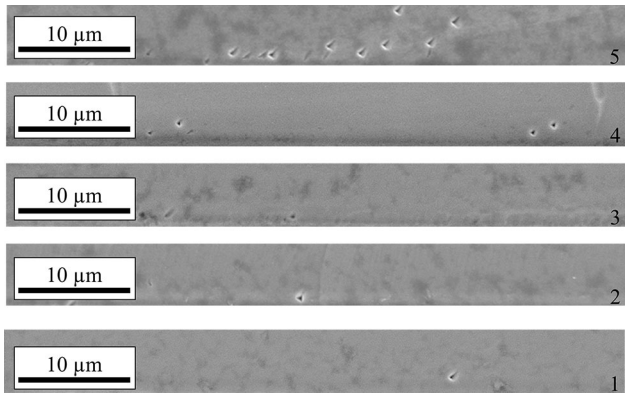

Fig. 3. Scanning electron microscopy micrographs measured on [01-1] face of LWIR $Hg_{1-x}Cd_xTe$ multilayer structures grown on (211)-oriented $Cd_{1-y}Zn_yTe$ substrates after a defect decoration etch. The micrographs are labeled 1 to 5 in order of increasing equivalent strain of the $Hg_{1-x}Cd_xTe$ multilayer structure with respect to the substrate. A pit indicates the presence of a dislocation.

micrographs are oriented such that the vertical direction on the page is along the growth axis. A pit indicates the presence of a dislocation. The dislocations tend to collect at a specific point of high excess stress in the structure, and at large mismatch their density increases and position spread throughout the structure. The quantitative dependence of the single-kink and misfit dislocation density on the degree of strain in the film was determined by measuring the linear etch pit density over an 800-μm span that overlapped the region of the film on which the x-ray diffraction measurements were performed. The correlation between the FWHM, the linear etch pit density, and the Zn composition of the substrate is depicted in Figs. 4 and 5, respectively. The Zn composition of the portions of material allocated for the measurements that resulted in Figs. 4 and 5 was known with less accuracy than the data in the preceding figures; the Zn composition was known to within the error indicated by the width of the data points in Fig. 5. Etch pits were also observed on the [1-11] face but at lower linear densities.

Etch pits on the same sections of wafers were measured on the (211) face using dark-field optical microscopy to determine the threading dislocation density. The etch pit densities varied between approximately 10^4 cm^{-2} and 5×10^4 cm^{-2}. Using this technique, a correlation between the FWHM and areal etch pit density or between the areal etch pit density and the Zn composition of the substrate was not observed.

Combining etch pit density measurements and strain measurements from symmetric and asymmetric reflection RSMs at select locations on wafers that nearly span the substrate Zn composition range in increments of less than or equal to 0.3% of the dataset in Fig. 2, the following was observed in regards to the active layer: The strain state appears to be finite at all substrate Zn compositions. A relatively small degree of shear and compressive

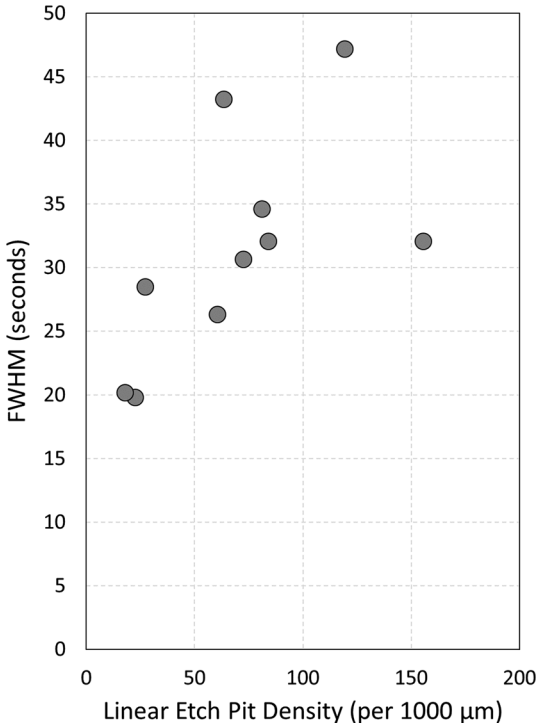

Fig. 4. Full-width at half-maximum of the surface symmetric (422) x-ray diffraction reflection versus the linear etch pit density measured on the [01-1] face of LWIR $Hg_{1-x}Cd_xTe$ multilayer structures. The linear etch pit density was measured over an 800-μm span overlapping the region of the film on which the x-ray diffraction measurements were performed.

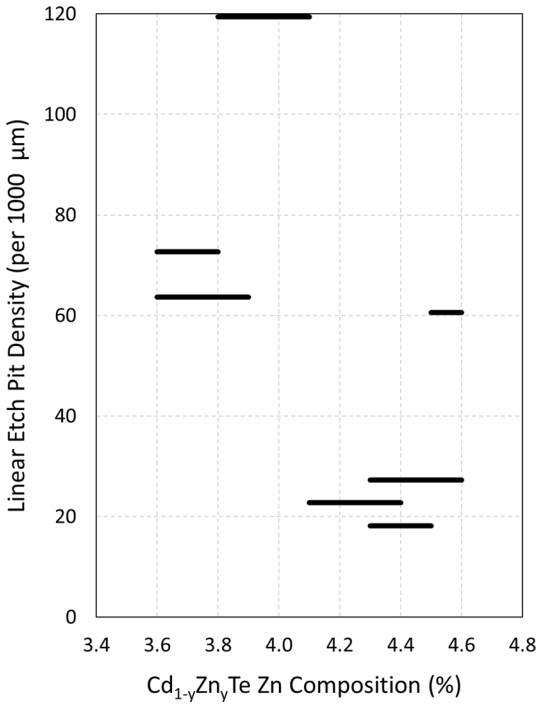

Fig. 5. Linear etch pit density measured on the [01-1] face of LWIR $Hg_{1-x}Cd_xTe$ multilayer structures versus the percent Zn composition of the (211)-oriented $Cd_{1-y}Zn_yTe$ substrates. The width of the data points indicates the uncertainty in the Zn composition of the wafer segment on which the linear etch pit density was measured.

or tensile strain is measured in the range of 4.2% to 4.4%. The strain outside of this region is also finite, even for regions where relaxation by the creation of extended defects took place. The degree of compressive strain was larger at substrate Zn composition of 4.4% and greater, while the degree of tensile strain was larger at substrate Zn composition of 4.2% and lower. At 4.4% and greater and 4% and lower, dislocations having a segment parallel to the growth surface of the film are not necessarily confined to an interface or plane. At 4.5% and greater and 3.8% and lower, dislocation clusters are observed. It is presumed that, in these clusters, the strain fields of individual dislocations are not isolated. At 3.5% and lower, a surface crosshatch pattern can be observed under Nomarski microscopy.

Together, these findings lead to the following interpretation of the dependence of the x-ray diffraction FWHM on the Zn composition of the substrate in Fig. 2: The smallest FWHM measured at a given substrate Zn composition is dictated by the degree of lattice matching between the multilayer structure and the substrate. The spread in FWHM values at a given substrate Zn composition may have the following causes: Measurement error in both the precision to which the substrate Zn composition is known at the location at which the properties of the $Hg_{1-x}Cd_xTe$ film were measured and variations in aligning the goniometer degrees of freedom may have led to an apparent spread in FWHM values at a given substrate Zn composition. Substrate crystal quality variations, such as local variations in the dislocation density, also may have led to a true spread in FWHM values at a given substrate Zn composition. The latter cause merits further investigation.

A key finding of this work is that, for the multilayer $Hg_{1-x}Cd_xTe$ structure under investigation, exceptionally high crystal quality was achieved when the range of substrate Zn composition was maintained to within ±0.1% of an optimum value of 4.3%. The high crystal quality of the epitaxial thin films is enabled by the high crystal quality of the underlying substrate. It is emphasized that, to maintain high-crystal-quality epitaxy, the substrate Zn composition areal variation needs to be held to within a fraction of a percent. The experimental methods and analysis that led to this finding can be generalized to optimize other multilayer structures to minimize relaxation by the generation of extended defects.

An important extension of this work would be the study of variations in the low threading dislocation density of $Cd_{1-y}Zn_yTe$ substrates and epitaxial $Hg_{1-x}Cd_xTe$ thin films by suitable nondestructive techniques. It is proposed that researchers in the field consider (1) a systematic study of x-ray diffraction reflection profiles on epi-layers and substrates, and (2) the application of electron channeling contrast imaging[20] to characterize dislocation character and density. The latter has been effective at characterizing dislocations in a variety of semiconductor systems[21,22] and could be suitable to study dislocations in certain $Hg_{1-x}Cd_xTe/Cd_{1-y}Zn_yTe$ heterostructures.

CONCLUSIONS

State-of-the-art $Hg_{1-x}Cd_xTe$ multilayer structures grown on (211)-oriented $Cd_{1-y}Zn_yTe$ substrates by MBE were characterized and their strain and relaxation analyzed. Techniques for measuring lattice mismatch, strain, and crystal quality by measuring symmetric and asymmetric diffraction profiles in different azimuths were adapted and performed in combination with dislocation delineation for full-wafer and multilayer characterization. It was found that the degree of lattice mismatch and in turn the strain state of epitaxial multilayers can be made uniform across full wafers in optimized structures. A strong correlation was revealed between the Zn composition of the $Cd_{1-y}Zn_yTe$ substrates and the crystal quality of the active layers in the multilayer structures. This method can be generalized to optimize multilayer structures to minimize relaxation by the generation of extended defects.

REFERENCES

1. M. Zandian, M. Farris, W. McLevige, D. Edwall, E. Arkun, E. Holland, J.E. Gunn, S. Smee, D.N.B. Hall, K.W. Hodapp, A. Shimono, N. Tamura, M. Carmody, J. Auyeung, and J.W. Beletic, Proceedings of SPIE 9915, High Energy, Optical, and Infrared Detectors for Astronomy VII, 99150F (2016).
2. D. Lee, M. Carmody, E. Piquette, P. Dreiske, A. Chen, A. Yulius, D. Edwall, S. Bhargava, M. Zandian, and W.E. Tennant, *J. Electron. Mater.* 45, 9 (2016).
3. S.M. Johnson, D.R. Rhiger, J.P. Rosbeck, J.M. Peterson, S.M. Taylor, and M.E. Boyd, *J. Vac. Sci. Technol., B* 10, 1499 (1992).
4. R.S. List, *J. Electron. Mater.* 22, 1017 (1993).
5. A.T. Paxton, A. Sher, M. Berding, M. Van Schilfgaarde, and M.W. Muller, *J. Electron. Mater.* 24, 52 (1995).
6. A. Szilagyi and M.N. Grimbergen, *J. Vac. Sci. Technol., A* 4, 2200 (1986).
7. M. Yoshikawa, K. Maruyama, T. Saito, T. Maekawa, and H. Takigawa, *J. Vac. Sci. Technol., A* 5, 3052 (1987).
8. M.A. Berding, W.D. Nix, D.R. Rhiger, S. Sen, and A. Sher, *J. Electron. Mater.* 29, 676 (2000).
9. M. Carmody, D. Lee, M. Zandian, J. Phillips, and J. Arias, *J. Electron. Mater.* 32, 710 (2003).
10. C. Fulk, T. Parodos, P. Lamarre, S. Tobin, P. LoVecchio, and J. Markunas, *J. Electron. Mater.* 38, 8 (2009).
11. J.H. van der Merwe, *J. Appl. Phys.* 34, 123 (1963).
12. J.Y. Tsao and B.W. Dodson, *Appl. Phys. Lett.* 53, 848 (1988).
13. J.Y. Tsao and B.W. Dodson, *Surf. Sci.* 228, 260 (1990).
14. M. Li, R. Gall, C.R. Becker, T. Gerhard, W. Faschinger, and G. Landwehr, *J. Appl. Phys.* 82, 4860 (1997).
15. S.M. Johnson, J.L. Johnson, W.J. Hamilton, D.B. Leonard, T.A. Strand, E.A. Patten, J.M. Peterson, J.H. Durham, V.K. Randall, T.J. deLyon, J.E. Jensen, and M.D. Gorwitz, *J. Electron. Mater.* 29, 680 (2000).
16. R.H. Sewell, C.A. Musca, J.M. Dell, L. Faraone, B.F. Usher, and T. Dieing, *J. Electron. Mater.* 34, 795 (2005).
17. T. Skauli, T. Colin, and S. Løvold, *J. Cryst. Growth* 172, 97 (1997). https://doi.org/10.1016/S0022-0248(96)00732-4.
18. W.L. Bond, *Acta Cryst.* 13, 814 (1960).

19. E.C. Piquette, M. Zandian, D.D. Edwall, and J.M. Arias, *J. Electron. Mater.* 30, 6 (2001).
20. A.J. Wilkinson, G.R. Anstis, J.T. Czernuszka, N.J. Long, and P.B. Hirsch, *Philos. Mag. A* 68, 59 (1993).
21. S.D. Carnevale, J.I. Deitz, J.A. Carlin, Y.N. Picard, D.W. McComb, M. De Graef, S.A. Ringel, and T.J. Grassman, *IEEE J. Photovolt.* 5, 676 (2015).
22. K. Mukherjee, B.A. Wacaser, S.W. Bedell, and D.K. Sadana, *Appl. Phys. Lett.* 110, 232101 (2017).